Research Square

Preprints are preliminary reports that have not undergone peer review.
They should not be considered conclusive, used to inform clinical practice,
or referenced by the media as validated information.

Green Biorefinery Approach for Taberau (Phragmites australis) Biomass: Delignification by Coriolopsis caperata and Bioethanol Production via MIL-100(Fe)–Immobilized Saccharomyces cerevisiae

Titin Apung Atikah
Universitas Palangka Raya
Yanetri Asi
Universitas Palangka Raya
Yuliana Yuliana
Universitas Palangka Raya
Wilson Jefriyanto
Universitas Palangka Raya
Lidya Tesalonika
Universitas Palangka Raya
Eka Jhonatan Krissilvio
Universitas Palangka Raya
Retno Agnestisia
retno.agnestisia@mipa.upr.ac.id

Universitas Palangka Raya

Research Article

Keywords: Bioethanol, immobilization, MIL-100(Fe), Phragmites australis

Posted Date: May 14th, 2026

DOI: https://doi.org/10.21203/rs.3.rs-9512742/v1

License: This work is licensed under a Creative Commons Attribution 4.0 International License.
Read Full License

Version of Record: A version of this preprint was published at Applied Biochemistry and Biotechnology on July 20th, 2026. See the published version at https://doi.org/10.1007/s12010-026-05827-2.

Abstract

This study explored bioethanol production from *Taberau*lignocellulosic biomass through fungal delignification, enzymatic hydrolysis, and fermentation using MIL-100(Fe)-immobilized yeast. The fungal pre-treatment with *Coriolopsis caperata*enhanced laccase activity, reaching a maximum of 520 U/L at 12 days, and significantly reduced lignin content from 20.87% to 10.92%. This reduction improved cellulose accessibility and increased the availability of fermentable sugars during hydrolysis. Enzymatic hydrolysis results showed that fungal-treated biomass produced higher reducing sugar concentrations compared to untreated and control samples, indicating effective lignin removal. Fermentation was conducted under various conditions, with optimal ethanol production achieved at a yeast dosage of 2% (w/v) and a fermentation time of 4 days, resulting in an ethanol concentration of 11.57 g/L. Characterization using FTIR, XRD, and SEM confirmed successful immobilization of yeast on MIL-100(Fe) without structural degradation. The immobilized system demonstrated improved stability and reusability compared to free yeast. The obtained ethanol concentration is within the typical range for SHF-based lignocellulosic bioethanol production. The integration of fungal pre-treatment with MOF-based immobilization provides a promising and sustainable strategy, with potential for further improvement through process optimization and alternative fermentation approaches.

Highlights

- Current perspective of bioethanol production from Taberau (*Phragmites australis*) Biomass
- Utilizing *Coriolopsis caperata*, a ligninolytic fungus from Central Kalimantan, for efficient hydrolysis of lignocellulosic biomass
- Improved performance of fermentation due to the action of immobilized yeast (*Saccharomises cerevisiae*).
- MIL-100(Fe) provided a robust platform for yeast immobilization, improving stability, reusability, and catalytic efficiency.

1. Introduction

Indonesia's heavy dependence on fossil fuels for energy poses a significant challenge. According to Hasan et al. (2012), fossil energy sources—petroleum (34.37%), coal (29.02%), and natural gas (23.49%)—dominate the nation's energy mix, while renewable energy contributes only about 11.95% [1]. Meanwhile, global energy demand is projected to rise by 45% by 2030, with an average annual growth rate of 1.6% [2]. However, fossil fuels are finite resources that will become increasingly scarce [3–5]. In addition to their finite availability, the combustion of fossil fuels contributes to environmental degradation through greenhouse gas emissions, thereby accelerating global warming [5–7]. These pressing challenges underscore the urgent need for sustainable, renewable energy alternatives to secure a cleaner, more resilient energy future.

One viable alternative is bioethanol, a renewable energy source with significant potential to transform the energy sector [6, 8, 9]. In particular, lignocellulosic biomass—non-food plant material—emerges as an ideal feedstock for second-generation (G2) bioethanol production [9, 10]. This biomass is rich in cellulose and hemicellulose, which can be converted into bioethanol through advanced processes [11, 12]. Persson (2018) highlighted that G2 bioethanol offers lower greenhouse gas emissions than conventional fossil fuels [13], making it a more sustainable and environmentally friendly option. However, scaling up G2 bioethanol production presents several challenges. The current efficiency of feedstock selection, biomass pre-treatment, and fermentation processes still falls short of what is required for widespread commercial viability [14]. Despite these obstacles, the potential of bioethanol as a sustainable, low-emission energy source has never been more promising.

Phragmites australis (locally known as *Taberau*), a weed species from the Poaceae family, has emerged as a promising lignocellulosic feedstock for G2 bioethanol production [15, 16]. Native to the peat swamp forests of Central Kalimantan, this plant is found in abundance but remains underutilized in the context of renewable energy applications. With its high cellulose and hemicellulose content [15–17], *Taberau* is considered a promising raw material for G2 bioethanol production using non-edible biomass sources. In addition to its favorable chemical composition, *Taberau* offers several other beneficial traits, such as rapid growth, high biomass yield, and minimal requirements for water and nutrients [16–19]. These characteristics position *Taberau* as a sustainable, low-impact biomass resource, aligning with the objectives of advancing biofuel technologies and and the transition toward more efficient and eco-friendly energy systems. However, utilizing lignocellulosic biomass effectively requires pre-treatment to remove lignin and facilitate the breakdown of cellulose and hemicellulose. Several pre-treatment methods have been developed, including base treatment [20], acid treatment [20, 21], organic solvent-based fractionation [19], and steam explosion [15, 16]. These methods often require the use of chemicals or extreme reaction conditions, which can lead to biomass degradation and the formation of enzymatic inhibitors that hinder the saccharification process at later stages [12]. Consequently, biological methods—particularly those utilizing white rot fungi—are increasingly being explored as an alternative. This method is advantageous because they do not rely on harsh chemicals or extreme conditions, making them more cost-effective and environmentally friendly [12, 22, 23].

Several studies have reported that white rot fungi are capable of lignin degradation by producing ligninolytic enzymes such as laccase, lignin peroxidase, and manganese peroxidase [12, 24–26]. Roth and Spiess [27] further emphasized that laccase is particularly effective for detoxifying phenolic fragments in delignified biomass, which can otherwise inhibit cellulolytic enzyme activity during the saccharification process at later stages. Numerous white rot fungi species have been employed for biomass delignification, including *Phanerochaete chrysosporium* [28], *Pleurotus eryngii, Irpex lacteus* [29], *Ganoderma lucidum, Pleurotus ostreatus, Pleurotus pulmonarius, Trametes sp.* [30], *and Pleurotus sajor-caju* [31]. *The white rot fungus Coriolopsis caperata, isolated from* the previous study, *has shown considerable laccase enzyme activity* [32, 33]. Therefore, biomass pre-treatment using *C. caperata* for the delignification process is considered a promising approach.

Furthermore, the Separate Hydrolysis and Fermentation (SHF) method, which decouples the hydrolysis of cellulose from the fermentation stages, has demonstrated significant potential for second-generation (G2) bioethanol production [34, 35]. In this process, cellulose is first converted into glucose through hydrolysis, followed by fermentation into ethanol by *Saccharomyces cerevisiae* (yeast) [34, 35]. The separation of these steps in the SHF process enables independent optimization of enzymatic hydrolysis and fermentation conditions, thereby enhancing overall efficiency and reducing the inhibitory impact of ethanol on cellulolytic enzymes [36]. Moreover, *S. cerevisiae* can be immobilized onto various support materials, which facilitates cell separation from the fermentation medium, reduces operational costs through cell reuse across multiple fermentation cycles, enhances cell stability, and decreases contamination risks and fermentation time [37, 38]. Common support materials for *S. cerevisiae* immobilization include sodium alginate [38, 39], calcium alginate [40], and CMC-g-PVP [41]. Recently, however, metal-organic frameworks (MOFs) have recently been recognized as promising platforms for the immobilization of *S. cerevisiae* [42, 43] and *Escherichia coli* [44, 45]. Among these MOFs, MIL-100(Fe) has attracted considerable attention due to its regular crystal structure, excellent stability, high surface area, non-toxicity, and biodegradability, making it an ideal candidate for yeast immobilization [46, 47]. Despite these advances, the optimization of the SHF method using *Taberau* biomass pre-treated with *Coriolopsis caperata* and MIL-100(Fe)-immobilized *S. cerevisiae* for bioethanol production has not yet been thoroughly investigated. The present research aims to bridge this gap by evaluating Taberau as a sustainable raw material for bioethanol production, enhanced by innovative pre-treatment and fermentation approaches.

2. Materials and Methods

2.1. Materials

The materials used in this study were iron (II) sulfate heptahydrate ($FeSO_4.7H_2O$), trimesic acid (H_3BTC), sodium hydroxide (NaOH), sodium acetate (CH_3COONa), acetic acid (CH_3COONa), veratryl alcohol ($(CH_3O)_2C_6H_3CH_2OH$), syringaldazine ($[HOC_6H_2(OCH_3)_2CH = N-]_2$), which were supplied by Merck. D-glucose ($C_6H_{12}O_6$), peptone, potassium dihydrogen phosphate (KH_2PO_4), dipotassium hydrogen phosphate (K_2HPO_4), zinc sulfate ($ZnSO_4$), iron(II) sulfate ($FeSO_4$), manganese (II) sulfate ($MnSO_4$), and magnesium sulfate (MgSO4) was used to prepare a glucose-peptone medium, while yeast extract, peptone, D-glucose ($C_6H_{12}O_6$), agar was used to prepare yeast extract peptone glucose (YPG) agar medium. 3,5-Dinitrosalicylic acid (DNS) reagent was used for estimating reducing sugar concentration. Distilled water was used as the solvent in all experiments.

2.2. Instrumentation

Structural analysis of samples was conducted using XRD (Philips PW1140/90). Finely ground and dried samples were mounted on the sample stage and analyzed over a 2θ range of 5–60° employing Cu-Kα radiation to assess crystallinity. Functional group characterization was carried out using FTIR (Shimadzu FTIR-8400S) with the KBr pellet method, covering a spectral range of 400–4000 cm^{-1}. In addition, the

surface morphology of the materials was examined using SEM equipped with an Advanced Microanalysis system.

2.3. Feedstocks

Taberau stems was harvested from the countryside of Lais Lake, Tanjung Sangalang Village, Central Kahayan District, Pulang Pisau Regency, Central Kalimantan, Indonesia. The harvested *Taberau* was air-dried for 2 days on the field, and ground until they passed a 60-mesh sieve. The sieved *Taberau* was subsequently dried until it reached a moisture content of 10%.

2.4. Organisms and culture maintenances

C. caperata was pre-cultured on potato dextrose agar (PDA, 39 g/L) plates at 27 ± 2°C for 7 days in the dark. Meanwhile, *S. cerevisiae* (yeast) cells maintained on YPG agar medium [39], was obtained from the available stock culture of Institut Pertanian Bogor Culture Collection (IPBCC), Bogor Indonesia. Slant media were incubated at 30°C over a period of 1–2 days to promote maximal growth.

2.5. Fungal inoculation

Ten agar plugs (5 mm in diameter) from the plate culture were aseptically introduced into 100 mL of glucose–peptone medium in a 250 mL Erlenmeyer flask to obtain the liquid culture. The glucose-peptone medium was prepared as previously reported by Agnestisia *et al.* [32]. The cultures were maintained at 27 ± 2°C without agitation in dark conditions for 16 days, with 1 mL of veratryl alcohol (100 mM) added after 2 days to promote laccase production. Liquid samples were collected every two days and blended to obtain a homogeneous inoculation. The laccase enzyme activity was then measured.

2.6. Fungal pre-treatment

Fungal pre-treatment assays were performed in triplicate using 250 mL Erlenmeyer flasks. Ten grams of *Taberua* biomass were conditioned with a phosphate buffer solution (pH 5) to achieve an initial moisture content of 75%. Moistened substrates underwent sterilization at 121°C for 30 minutes. After cooling, each flask received 5 mL of a homogeneous liquid culture with the highest laccase activity and was subsequently incubated without agitation at 27 ± 2°C for 35 days. The flasks were sealed with sterile, non-absorbent cotton to allow air exchange between the atmosphere and the culture. A control, consisting of 2 mL of acetate buffer solution instead of fungal inoculation, was also included for each biomass sample. The biomass was then washed after fungal pre-treatment. The contents of cellulose, hemicellulose-associated carbohydrates, and lignin in raw, control, and fungal-treated feedstocks were quantified via a gravimetric method.

2.7. Enzymatic hydrolysis

Five grams of cellulase (CAS 9012-54-8, with activity of 20,000 U/g) were added to 500 mL of a 1% (w/v) substrate (raw, control, and fungal-treated feedstocks, respectively) in acetate buffer (pH = 4.8, 50 mM) and stirred at 50°C for 10, 30, 50, 70, and 90 min. The hydrolysis solution was then used to estimate reducing sugar concentration.

2.8. Preparation of yeast cell suspension

Ten milliliters of sterile distilled water were added to a 24-hour-old slant culture of *S. cerevisiae*, after which the cells were aseptically scraped using a sterile inoculating needle and gently agitated to obtain a uniform suspension. Subsequently, 100 mL of YPG medium (agar-free) were dispensed into 250 mL Erlenmeyer flasks, plugged with cotton, sterilized, and cooled to room temperature. Each flask were inoculated with 1 mL of cell suspension under aseptic conditions and incubated at 30°C with shaking at 150 rpm for 24 h. Cells were harvested by centrifugation (6000 rpm, 15 min), washed with saline, and re-centrifuged for an additional 5 min. The supernatant was removed, and the pellet was washed with saline solution, followed by an additional centrifugation step for 5 minutes. The final pellet was subsequently washed, air-dried, and weighed, and these cells were designated as free cells.

2.9. Immobilization of yeast cells

MIL-100(Fe) was synthesized in situ at room temperature by mixing an aqueous $FeSO_4 \cdot 7H_2O$ solution (3.8 g, 13.7 mmol in 120 mL) with an alkaline H_3BTC solution (1.9 g, 9.1 mmol in 30 mL of 1 M NaOH) under stirring (200 rpm). The precursor solution was added dropwise, and the mixture was stirred for 24 h. The resulting solid was washed with warm water and methanol, then dried at 60°C for 12 h. For immobilization, free yeast cells (0.25 g) were combined with MIL-100(Fe) (0.25 g) in acetate buffer (125 mL, 50 mM, pH 4.8). The immobilized cells were recovered by centrifugation (6000 rpm, 15 min), washed three times, air-dried for 24 h, and denoted as MIL-100(Fe)@yeast.

2.10. Ethanol fermentation

The ethanol fermentation of the *Taberau* hydrolysis solution in this study was conducted using a batch fermentation method. The effects of yeast dosage and fermentation time on ethanol production were investigated. MIL-100(Fe)@yeast and yeast cell free (2% w/v) were inoculated into 500 mL Erlenmeyer flasks containing 100 mL of sterilized liquid medium (pH 5), consisting of 0.15% yeast extract, 0.25% NH_4Cl, 0.55% K_2HPO_4, and 0.025% $MgSO_4 \cdot 7H_2O$, along with hydrolysis solution as the carbon source. The MIL-100(Fe)@yeast and yeast cell free systems were incubated at 30°C with agitation at 75 rpm for 4 hours. To assess the impact of yeast dosage and fermentation time, experiments were carried out with different MIL-100(Fe)@yeast and yeast cell free concentrations (0.5%, 1%, 1.5%, 2%, and 2.5% w/v) and fermentation durations (1 to 10 days). After the fermentation process, the MIL-100(Fe)@yeast and yeast cell free cells were separated from the fermented medium and stored for use in subsequent experiments. The fermented medium was then analyzed for ethanol and residual reducing sugar concentration.

2.11. Reusability of immobilized yeast cells

The reusability of MIL-100(Fe)@yeast was tested by performing multiple fermentation cycles. After each batch, the MIL-100(Fe)@yeast were recovered from the fermentation medium by filtration or centrifugation. The recovered cells were washed with sterile water to remove residual fermentation by-products and medium components. The washed MIL-100(Fe)@yeast were then reused in subsequent

fermentation cycles. The reuse experiments were carried out for up to six consecutive batches. In each cycle, the ethanol yield and glucose consumption were monitored, and the same procedure (as described above) was followed for each batch. Samples were drawn at regular intervals (every 24 hours) to measure ethanol content and sugar consumption.

2.12. Analytical methods

Laccase activity was assayed via syringaldazine oxidation [48] in a 3 mL system containing sodium tartrate buffer (0.1 M, pH 5.3), syringaldazine (0.5 mM), and enzyme solution. The increase in absorbance at 525 nm ($\varepsilon 525 = 65{,}000\ M^{-1}\cdot cm^{-1}$) was monitored for 2 min using a UV–Vis spectrophotometer. Furthermore, the concentration of reducing sugars was analyzed by the DNS method [49], with absorbance recorded at 540 nm using a UV–Vis spectrophotometer and quantified against a glucose standard curve. Ethanol content was determined by acid dichromate oxidation, where ethanol in a known sample mass was oxidized to acetic acid using 0.1 N potassium dichromate in the presence of sulfuric acid. In addition, the physical properties of distilled ethanol from this study consisting of density, viscosity, specific gravity, API specific gravity, and flash point, were also determined. Specific gravity was determined using the ASTM D 792 – 13 method. Viscosity was analyzed using a Saybolt viscosimeter with the ASTM D 88 test standard. Flash point were determined using a flash and fire point tester with the ASTM D 92 test standard. Specific gravity and API gravity were analyzed using the ASTM D 891-09 and ASTM D 287 test standards, respectively.

3. Results

3.1. Fungal laccase enzymes

The fungal inoculation method used in this study successfully facilitated the production of laccase enzymes, with a particular focus on examining the effects of incubation period on laccase activity generated by *C. caperata* (Fig. 1). Determining the optimal incubation time is crucial for maximizing laccase production in the shortest time possible. To achieve this, incubation times were varied across a range of 2, 4, 6, 8, 10, 12, 14, and 16 days. This range was selected to assess early metabolic activity and temporal fungal performance, enabling evaluation of laccase production stability and nutrient-related effects. Similar incubation timeframes have been employed in previous studies on laccase production in other fungi, such as *Ganoderma* sp. [50], *Trametes versicolor* [51], and *Trametes trogii* [52]. The data obtained from these varied incubation periods will contribute to optimizing laccase production and provide a better understanding of its efficiency over time.

The *C. caperata* fungal culture appeared to show stable growth, and the addition of 1 mL of 100 mM veratryl alcohol after two days of incubation significantly enhanced laccase production. The enzyme activity increased steadily after the second day, reaching an optimum at 12 days with an enzyme activity of 520 U/L, and then declined towards the end of the incubation period, likely due to nutrient depletion or a reduction in fungal metabolic activity. The laccase enzyme activity of *C. caperata* appeared to be lower than that of *C. caperata* BM-172 (880 U/L) [53], but is higher compared to other white rot fungi, such as

Fuscoporia gilva (440 U/L) and *Pleurotus tuberregium* (480 U/L) [23]. Therefore, *C. caperata* is considered to have the potential to be used as a delignification agent for Taberua biomass in this study.

3.2. Delignification of *Taberau* biomass

Fungal pre-treatment assays conducted on *Taberua* biomass showed significant delignification, as indicated by the reduction in lignin content following fungal inoculation (Table 1). A control group, using acetate buffer instead of the fungal inoculum, was included to isolate the effect of the fungal treatment. The most notable observation in this study was the significant reduction in lignin content in the fungal-treated feedstock (10.92% ± 1.15%), compared to the raw feedstock (20.87% ± 0.82%) and the control feedstock (19.35% ± 0.74%). This reduction in lignin content is consistent with the known role of laccase-producing fungi in delignification processes. Laccases, a group of enzymes produced by certain fungi, have been widely recognized for their ability to oxidize lignin, breaking down its complex aromatic structure into smaller fragments. The marked decrease in lignin content following fungal treatment provides strong evidence that fungal inoculation, particularly through laccase activity, was the primary mechanism responsible for the observed delignification. This delignification process also enhanced the availability of cellulose and holocellulose -associated carbohydrates, making the biomass more accessible for further biochemical conversion processes such as enzymatic hydrolysis [54]. These findings align with previous studies in which fungal treatments using laccase-producing fungi facilitated lignin degradation and improved the accessibility of polysaccharides [29, 30, 54, 55].

Table 1
Chemical composition of feedstocks

Composition (%)	Raw feedstock	Control feedstock	Fungal-treated feedstock
α-Cellulose	39.24 ± 0.47	38.24 ± 1.67	45.21 ± 1.04
Holocellulose	56.68 ± 0.75	59.20 ± 0.85	60.68 ± 0.52
Lignin	20.87 ± 0.82	19.35 ± 0.74	10.92 ± 1.15

Furthermore, the control group in this study, which used acetate buffer instead of fungal inoculum, did not exhibit significant changes in biomass composition, reinforcing the notion that laccase activity was the key driver behind the observed delignification. This finding is consistent with prior research, which also reported no significant changes in biomass composition in the absence of fungal inoculation, confirming the effectiveness of laccase-producing fungi in biomass pre-treatment [54]. By degrading lignin, the fungal treatment enhances the overall porosity and accessibility of the biomass, thus improving the efficiency of downstream processes like enzymatic hydrolysis, which is crucial for converting the polysaccharides into fermentable sugars for bioethanol production.

3.3. Enzymatic hydrolysis

Enzymatic hydrolysis was performed to assess the sugar release potential from raw, control, and fungal-treated feedstock. The hydrolysis reaction was carried out at 50°C for various time intervals (10, 30, 50, 70, and 90 minutes). The results presented in Fig. 2 demonstrate that fungal pre-treatment significantly enhances the enzymatic hydrolysis of *Taberua* feedstock, as evidenced by the higher sugar release from fungal-treated feedstock compared to raw and control feedstocks. The fungal pre-treatment, which effectively degraded lignin, made the cellulose more accessible to cellulase enzymes, leading to a marked increase in sugar yield after 50 minute of hydrolysis. This finding aligns with several other studies that have shown similar improvements in sugar release following lignin removal through fungal inoculation. For instance, studies by Gupta et al. (2011) demonstrated that laccase-producing fungi can efficiently break down lignin, enhancing the accessibility of cellulose and improving the efficiency of enzymatic hydrolysis [56]. In contrast, the raw and control samples, which retained most of their lignin, exhibited slower sugar release, particularly at earlier time points, confirming the protective role of lignin in impeding cellulase action. This observation is consistent with several researcher that reported lignin removal is crucial for optimizing biomass conversion processes [12, 24, 56]. Overall, the results emphasize the effectiveness of fungal pre-treatment in improving the efficiency of biomass hydrolysis, offering a promising strategy for enhancing biofuel production and other biotechnological applications.

3.4. MIL-100(Fe) Immobilized yeast cells

The synthesis of MIL-100(Fe) and the immobilization of yeast cells onto this material were performed. MIL-100(Fe) was prepared via an in situ method at room temperature [57], after which the obtained material was utilized as a support for yeast immobilization, yielding MIL-100(Fe)@yeast. Both MIL-100(Fe) and MIL-100(Fe)@yeast were subsequently characterized using FTIR, XRD, and SEM to confirm the successful synthesis and immobilization processes. FTIR analysis was conducted to identify functional groups and to verify the presence of characteristic MOF bonds as well as potential interactions between yeast cells and the MIL-100(Fe) framework.

The immobilization of yeast cells onto the material were successfully carried out using an in situ method at room temperature. This method enables the formation of a stable MOF structure while providing a suitable surface for biological immobilization. MIL-100(Fe) is widely reported as a robust MOF with high surface area and excellent chemical stability, making it highly suitable for hosting biomolecules and microbial cells [42, 43, 58].

The FTIR spectra of MIL-100(Fe) and MIL-100(Fe)@yeast, recorded in the range of 400–4000 cm^{-1}, exhibit very similar spectral patterns (Fig. 3). This indicates that the immobilization process does not significantly affect the structural integrity of the MIL-100(Fe) framework. Characteristic absorption bands such as O–H stretching (~ 3400–3500 cm^{-1}), C = O stretching (~ 1625–1635 cm^{-1}), and Fe–O vibrations (~ 600–630 cm^{-1}) remain clearly visible after immobilization. These findings are consistent with previous reports showing that MIL-100(Fe) maintains its structural framework even after chemical modification or interaction with external species [59, 60]. The preservation of these functional groups suggests that the coordination between Fe^{3+} ions and the organic ligands remains intact. According to

Han et al. (2017), the stability of MIL-100(Fe) originates from its strong metal–ligand coordination and mesoporous architecture, which provides resistance against structural collapse during post-synthetic modification [60]. This characteristic is crucial for applications involving biological systems, where mild conditions are typically required.

In addition to the characteristic peaks of MIL-100(Fe), the FTIR spectrum of MIL-100(Fe)@yeast shows additional absorption bands that can be attributed to yeast cells in Fig. 3. The absorption peak at approximately 2926 cm^{-1} corresponds to C–H stretching vibrations of aliphatic groups, while the band at around 1572 cm^{-1} is associated with amide groups from proteins. These functional groups are typical components of microbial cells, including proteins and lipids, confirming the successful immobilization of yeast onto the MOF surface [61]. Furthermore, the presence of a band near 1047 cm^{-1}, corresponding to C–O stretching vibrations, indicates the presence of carbohydrates such as polysaccharides in the yeast cell wall. Yeast cell walls are primarily composed of glucans, mannoproteins, and chitin, which contribute to these characteristic FTIR signals [61]. The detection of these functional groups suggests that the yeast cells maintain their structural integrity and biochemical composition after immobilization.

The coexistence of MIL-100(Fe) characteristic peaks and yeast-related bands indicates that the immobilization process occurs mainly through surface interactions, such as hydrogen bonding and electrostatic interactions, rather than through structural disruption. Similar observations have been reported in previous studies, where MOFs served as effective supports for enzyme and microbial immobilization without compromising their activity [42, 43, 58, 62].

To further strengthen the identification results obtained from FTIR for MIL-100(Fe) and MIL-100(Fe)@yeast, additional supporting data in the form of XRD analysis is necessary. This data is expected to determine the crystallinity of the MIL-100(Fe) material. It is important to ensure that MIL-100(Fe) was successfully synthesized and retained its structural integrity after the yeast cell immobilization process. The XRD patterns would also reveal any changes in crystallinity due to the incorporation of yeast cells into the framework. The diffraction peaks observed in the XRD patterns of MIL-100(Fe) and MIL-100(Fe)@yeast correspond to the characteristic crystal lattice planes of the analyzed materials (Fig. 4). According to the JCPDS, distinct peaks at 2θ values of 6.08°, 10.22°, and 10.98° are indicative of MIL-100(Fe). These reflections confirm the successful formation of MIL-100(Fe) and the retention of its crystallinity throughout the synthesis process.

A comparison of the diffractogram of MIL-100(Fe) with that of MIL-100(Fe)@yeast reveals that the immobilization of yeast cells on the MIL-100(Fe) surface does not significantly alter the overall crystalline structure of the material. The XRD pattern of MIL-100(Fe)@yeast exhibits almost identical diffraction peaks to those of MIL-100(Fe), suggesting that the framework of the MOF remains intact after the immobilization process. However, a notable difference is the appearance of a new peak at 2θ = 20.63°, which is characteristic of yeast. This additional peak is attributed to the specific diffraction pattern of the yeast cells, indicating that they have been successfully incorporated into the MIL-100(Fe) structure. The appearance of this new peak supports the conclusion that yeast cells are effectively

immobilized on the MIL-100(Fe) surface, without compromising the material's structural integrity. The persistence of the characteristic MIL-100(Fe) peaks along with the emergence of the yeast-specific peak further validates the stability and robustness of the immobilization process. These findings are consistent with the FTIR results, which also indicated that the yeast cells maintain their functional characteristics after immobilization. As the results, the XRD analysis complements the FTIR data and provides valuable confirmation that the immobilization of yeast cells on MIL-100(Fe) does not disrupt the material's crystalline structure. This dual validation from both FTIR and XRD techniques reinforces the potential of MIL-100(Fe) as a stable and effective platform for future biocatalytic applications, where the integrity of both the support material and the immobilized cells is crucial.

SEM analysis was further applied to examine the cross-sectional morphology and the distribution of synthesized MIL-100(Fe) (Fig. 5). The synthesized MIL-100(Fe) exhibited an octahedral particle shape, with crystallite sizes ranging from 100 nm to 2 μm, consistent with the sizes reported in the literature. However, the size and shape of the MIL-100(Fe) crystals were not uniform, which is typical for materials synthesized at room temperature. This variation in particle size is acceptable, as the synthesis was carried out under mild conditions. In contrast, when high-temperature synthesis methods are used, more homogeneous MIL-100(Fe) crystals can be produced due to better control over nucleation and crystal growth, resulting in more uniform particle size and shape.

Furthermore, SEM analysis of MIL-100(Fe)@yeast provides additional insight into the immobilization process. The micrographs show a clear morphological difference between MIL-100(Fe) and MIL-100(Fe)@yeast. The pristine MIL-100(Fe) exhibits irregular agglomerated particles, which is typical for this class of MOFs due to their high surface energy and porous structure. After immobilization, the MIL-100(Fe)@yeast sample shows increased aggregation and the formation of larger clustered structures. This change in morphology indicates the interaction between the MOF particles and the biological component. However, the distinct morphology of yeast cells, which are typically oval-shaped in *Saccharomyces cerevisiae*, is not clearly observed in the SEM images. This may be attributed to the coverage or partial encapsulation of yeast cells by MIL-100(Fe) particles, which can obscure their natural morphology. Such phenomena have been widely reported, as microorganisms or enzymes immobilized within porous supports or MOFs often become difficult to visually distinguish due to tight coating, encapsulation within pore structures, or strong host–guest interfacial interactions that obscure clear morphological boundaries between the biological entities and the supporting material [43, 63]. In addition, the cell wall of *Saccharomyces cerevisiae*, which is rich in polysaccharides and proteins, can promote adhesion to solid supports through hydrogen bonding and electrostatic interactions, further facilitating the immobilization process [61, 64].

Importantly, although individual yeast cells are not distinctly visible, the observed increase in particle size and aggregation strongly suggests successful immobilization. These SEM results are consistent with the FTIR and XRD analyses, which confirm the presence of biological functional groups and the preservation of the MIL-100(Fe) crystalline structure. The combination of these characterization

techniques provides complementary evidence that yeast cells have been successfully immobilized onto the MIL-100(Fe) framework without structural degradation.

3.5. Ethanol fermentation

The ethanol fermentation of *Taberau* hydrolysate using both MIL-100(Fe)@yeast and free yeast systems was evaluated at different yeast dosages. The results clearly demonstrate that yeast dosage significantly affects both sugar consumption and ethanol production (Fig. 6). For both systems, increasing yeast dosage from 0.5% to 2.0% (w/v) resulted in a marked increase in sugar consumption and ethanol production. In the MIL-100(Fe)@yeast system, sugar consumption increased from 16.07 g/L to 27.63 g/L, accompanied by an increase in ethanol concentration from 6.90 g/L to 11.30 g/L. A similar trend was observed in the free yeast system, although at lower levels, where sugar consumption increased from 14.20 g/L to 24.80 g/L, and ethanol production from 6.00 g/L to 10.17 g/L. The maximum ethanol production in both systems was achieved at a yeast dosage of 2%, suggesting an optimal balance between cell concentration and substrate availability. This observation is consistent with previous reports indicating that appropriate yeast loading enhances substrate utilization and ethanol productivity, whereas excessive biomass does not necessarily lead to higher yields [65].

Furthermore, the MIL-100(Fe)@yeast system consistently exhibited higher sugar consumption and ethanol production compared to free yeast. This can be attributed to the advantages of cell immobilization, which include improved cell stability, higher cell density, and increased resistance to inhibitory compounds. Immobilized yeast systems have been reported to achieve higher ethanol yields and maintain stable fermentation performance [38, 64, 66, 67]. However, further increasing the yeast dosage to 2.5% did not result in additional improvement. In both systems, sugar consumption decreased slightly, and ethanol production either plateaued or decreased. This indicates the existence of a threshold yeast concentration beyond which fermentation efficiency no longer improves. The decline at higher yeast loading can be attributed to cell overcrowding, competition for nutrients, and accumulation of inhibitory metabolites [68].

Fermentation time also plays a critical role in determining ethanol production efficiency. In this study, both sugar consumption and ethanol production increased significantly from day 1 to day 4 in both MIL-100(Fe)@yeast and free yeast systems (Fig. 7). In the MIL-100(Fe)@yeast system, sugar consumption increased from 16.53 g/L (day 1) to 27.77 g/L (day 4), accompanied by a rise in ethanol concentration from 5.60 g/L to 11.57 g/L. A similar trend was observed for free yeast, although at lower levels, where sugar consumption increased from 13.37 g/L to 24.40 g/L, and ethanol production from 3.50 g/L to 9.83 g/L over the same period. These results indicate that the active fermentation phase occurred within the first four days, during which yeast cells efficiently converted fermentable sugars into ethanol. This pattern is consistent with previous studies reporting that ethanol production typically increases during the exponential growth phase and reaches a maximum before entering the stationary phase [65].

The highest ethanol production for both systems was observed on day 4, confirming that this duration represents the optimum fermentation time. After day 4, both ethanol production and sugar consumption

showed a gradual decline. In the MIL-100(Fe)@yeast system, ethanol decreased from 11.57 g/L (day 4) to 9.63 g/L (day 10), while in the free yeast system it decreased from 9.83 g/L to 5.83 g/L. This decline suggests that most fermentable sugars had been consumed and that inhibitory effects, particularly from accumulated ethanol and metabolic by-products, began to negatively affect yeast activity. Similar observations have been reported in ethanol fermentation studies, where product inhibition and substrate depletion limit further ethanol production [68].

Compared to free yeast, the MIL-100(Fe)@yeast system consistently exhibited higher sugar utilization and ethanol production across all fermentation times. Additionally, the decline after the optimum point was less pronounced in the immobilized system, indicating better stability and resistance to inhibitory conditions. This behavior is characteristic of immobilized yeast systems, where the supporting matrix enhances cell protection, maintains higher cell density, and prolongs metabolic activity [38, 64, 66, 67]. Furthermore, immobilization has been widely reported to improve ethanol productivity and operational stability in lignocellulosic fermentation systems. These findings confirm that a fermentation duration of 4 days is optimal under the studied conditions. Extending fermentation beyond this point does not improve ethanol yield and may reduce efficiency due to substrate depletion and ethanol inhibition, as widely discussed in bioethanol production literature [38, 64, 66, 67].

3.6. Reusability of immobilized yeast cells

The reusability of MIL-100(Fe)@yeast over six consecutive fermentation cycles showed a progressive decrease in ethanol yield with each reuse, which is a common phenomenon observed in many immobilized enzyme and cell systems (Fig. 8). Our results indicate that ethanol yield decreased after each cycle, likely due to a combination of factors, including the decline in yeast cell viability, the gradual breakdown of the immobilization matrix, and the accumulation of inhibitory byproducts such as ethanol. In other study, the ethanol yield dropped after four cycles, which was attributed to both cellular stress and matrix degradation [39]. Similarly, in our study, the rate of decline in ethanol yield accelerated after the third cycle, suggesting that the yeast cells' metabolic capacity and structural integrity were compromised over time.

The results of this study showed a slight decrease in ethanol production after the second reuse cycle of immobilized yeast cells; however, this change was not statistically significant. This trend suggests that the immobilized system maintained relatively stable activity over repeated use, although minor variations may be associated with factors such as gradual loss of cell viability or partial nutrient depletion within the immobilization matrix. Similarly, Onaifo et al. (2016) reported no significant reduction in ethanol yield over successive reuse cycles. Minor differences between the studies may be attributed to variations in experimental conditions, particularly the immobilization strategies employed. For instance, the support material used by Onaifo et al. (2016) may have provided a more protective microenvironment for the yeast cells [69]. Additionally, differences in immobilization parameters, such as cell loading density or entrapment technique, could also contribute to the observed variations. These findings emphasize the importance of optimizing immobilization systems to enhance the stability and reusability of yeast for industrial bioethanol production.

3.7. Ethanol physical characterization

The physical properties of the distilled ethanol produced in this study were analyzed, and the results indicate that the ethanol meets key specifications commonly required for industrial applications (Table 2). The density of 0.812 g/cm³ is in close agreement with typical values for pure ethanol, which range from 0.789 g/cm³ to 0.792 g/cm³ at 20°C. This suggests that the ethanol produced is of high purity, with minimal impurities that could affect its density. The specific gravity of 0.827 is also consistent with standard ethanol, indicating that the ethanol produced is comparable to commercially available ethanol in terms of its physical composition and suitability for biofuel applications.

The viscosity of 1.65 mm²/s is within the range typically observed for ethanol (1.2–1.5 mm²/s at 20°C), which is relatively low compared to other liquids like oils or water. This moderate viscosity is advantageous for transportation and handling, as it facilitates pumping and mixing without significant resistance to flow. However, it also suggests that some dissolved impurities or fermentation by-products might slightly increase the viscosity, though it remains within acceptable limits for most industrial processes. The API specific gravity value of 42.90 further confirms the ethanol's suitability for fuel blending, particularly in the production of bioethanol as an alternative fuel. This value, a standard measure of a liquid's density relative to water, positions the ethanol produced in this study within the typical range expected for fuel-grade ethanol, which is essential for its use in the automotive industry and other energy applications. The flash point of 14°C, consistent with the flash point of pure ethanol (around 12–14°C), highlights the highly flammable nature of the product. This property is crucial for handling and storage, as ethanol's volatility makes it prone to ignition at relatively low temperatures. Therefore, proper safety precautions and storage conditions are required to mitigate risks in large-scale applications

Table 2
The physical properties of the distilled ethanol

Parameter	Value
Density (g/cm³)	0.812
Viscosity ((mm^2/s)	1.65
Specific gravity	0.827
API specific gravity	42.90
Flash point (°C)	14.00

When compared to other studies, the ethanol produced in this study shows similar physical properties to those reported in the literature. For instance, [69] reported an ethanol density of 0.79–0.81 g/cm³, viscosity between 1.4–1.7 mm²/s, and flash points in the range of 12–15°C, which are all within the values observed in our study. This consistency suggests that the fermentation process in our study was

both efficient and effective, producing ethanol with standard characteristics suitable for industrial and biofuel applications. The produced ethanol conforms to established bioethanol standards; however, further optimization of fermentation conditions remains necessary. Although flash point and viscosity are within acceptable limits, fine-tuning parameters such as pH and temperature could enhance purity and reduce residual components affecting ethanol quality. In addition, research into different immobilization techniques for yeast cells or the use of various protective additives could improve the yield and purity of ethanol, ensuring that the physical characteristics remain consistent over extended production cycles.

4. Discussion

The ethanol concentration obtained in this study (11.57 g/L) can be classified as moderate for lignocellulosic bioethanol production using SHF process. This value falls within the commonly reported range of 10–25 g/L for lignocellulosic substrates, indicating that the overall process performed reasonably well under the applied conditions. However, the yield did not reach higher levels typically associated with optimized or industrial-scale systems (> 40 g/L), which may be attributed to the presence of lignin-derived inhibitory compounds and the intrinsic limitations of the SHF process[36, 65].

The moderate ethanol yield obtained in this study is largely influenced by upstream processes, especially fungal delignification and enzymatic hydrolysis.. As shown in Section 3.1, laccase production by C. caperata reached its maximum at 12 days, indicating strong oxidative capability toward lignin degradation. This enzymatic activity played a key role in reducing lignin content from 20.87% to 10.92% (Table 1), as discussed in Section 3.2. The substantial lignin removal enhanced cellulose accessibility, which was further reflected in the improved sugar release during enzymatic hydrolysis (Section 3.3). The hydrolysis profile (Fig. 2) showed a clear increase in reducing sugar concentration up to the optimum reaction time, confirming that fungal pretreatment effectively disrupted the lignocellulosic matrix. However, despite this improvement, the remaining lignin fraction (~ 10%) and its derived compounds likely still imposed partial inhibition on both enzymatic and fermentation processes.

In lignocellulosic systems, residual lignin and its degradation products, such as phenolic compounds, furfural, and hydroxymethylfurfural (HMF), are known to inhibit both enzymatic hydrolysis and microbial fermentation. These compounds can disrupt yeast cell membranes, inhibit key metabolic enzymes, and reduce ethanol productivity [70]. Thus, even though fungal delignification significantly improved biomass accessibility, it may not have completely eliminated inhibitory effects, which explains the moderate ethanol yield obtained. To better contextualize these findings, a comparison with previous studies is presented in Table 3.

As shown in Table 3, the ethanol yield obtained in this study (11.57 g/L) falls within the range reported for lignocellulosic bioethanol production using the SHF process. Lower ethanol concentrations, such as 9.45 g/L from rice straw, have been reported for substrates treated with alkali–enzymatic methods, whereas higher values (30–31 g/L) were achieved from sweet sorghum bagasse and Douglas-fir

following steam pretreatment [71, 72]. Intermediate ethanol yields were also observed in cassava stems subjected to microwave-assisted alkali and acid pretreatments (13.66–17.84 g/L) [73]. These variations indicate that ethanol production is strongly influenced by the type and severity of pretreatment. More intensive methods, such as steam pretreatment and chemical delignification, generally enhance cellulose accessibility and lead to higher ethanol yields, but they may also increase the formation of inhibitory compounds. In contrast, the fungal delignification approach employed in this study represents a milder and more environmentally friendly strategy. This method effectively reduces lignin content while preserving carbohydrate fractions, although it may result in slightly lower ethanol production compared to more aggressive pretreatment techniques. Interestingly, the ethanol yield obtained in this study is comparable to that reported for sugarcane bagasse using Ca-alginate immobilized yeast (11.8 g/L) [72], highlighting that the performance of the MIL-100(Fe)-immobilized yeast system is within the expected range for SHF-based lignocellulosic fermentation.

Table 3
Comparison of lignocellulosic bioethanol production under different conditions

Biomass	**Pretreatment / Delignification**	**Yeast System**	**Method**	**Ethanol (g/L)**
Rice straw [71]	Alkali + enzymatic treatment	Free yeast	SHF	9.45
Sweet sorghum bagasse [72]	Steam pretreatment	Free yeast	SHF	31.20
Douglas-fir [72]	Steam pretreatment	Free yeast	SHF	30.20
Cassava stems [73]	Microwave-assisted alkali (3% NaOH)	Free yeast	SHF	17.84
Cassava stems [73]	Microwave-assisted acid (0.1 M H_2SO)	Free yeast	SHF	13.66
Taberau stems (this study)	Fungal delignification	MIL-100(Fe)-immobilized yeast	SHF	11.57
Sugarcane bagasse [74]	Microwave-assisted alkali (2.75% NaOH)	Ca-alginate beads-immobilized yeast	SHF	11.8

The effect of yeast dosage further highlights the importance of process optimization. Ethanol production increased significantly with increasing yeast concentration up to 2% (w/v), beyond which no substantial improvement was observed. This trend reflects the balance between microbial activity and substrate availability. At optimal conditions, yeast metabolism is maximized, allowing efficient conversion of fermentable sugars produced during hydrolysis. However, excessive yeast loading can lead to mass transfer limitations and increased competition for nutrients [68].

Fermentation time also played a decisive role, with maximum ethanol production observed at 4 days. This corresponds to the active metabolic phase of yeast, during which sugar consumption and ethanol

formation are at their peak. The decline observed at longer fermentation times is consistent with substrate depletion and ethanol inhibition. Importantly, this trend aligns with the hydrolysis behavior, where sugar availability is time-dependent, indicating that synchronization between hydrolysis and fermentation is critical in SHF systems. A key advantage of this study lies in the application of MIL-100(Fe)-based immobilized yeast, as discussed in Section 3.4. Characterization results (FTIR, XRD, and SEM) confirmed that yeast cells were successfully immobilized without disrupting the structural integrity of the MIL-100(Fe) framework. The presence of functional groups associated with yeast cells, along with the preservation of MOF crystallinity, indicates that immobilization occurred through surface interactions rather than structural modification. This stable immobilization likely contributed to improved fermentation performance by enhancing cell stability, protecting cells from inhibitory compounds, and maintaining a high local cell density.

Furthermore, MIL-100(Fe), with its porous structure and high surface area, supports yeast metabolic activity by enabling efficient substrate diffusion and enhanced mass transfer. These characteristics explain the superior performance of immobilized yeast compared to free yeast systems, as also reported in previous studies [38, 64, 66, 67]. The recycle experiments further demonstrated the practical advantages of immobilization. Ethanol production remained relatively high during the initial cycles and gradually decreased with repeated use. This decline can be attributed to cell leakage, partial deactivation, or structural changes in the immobilization matrix. Nevertheless, the ability to reuse the immobilized system highlights its potential for cost-effective and sustainable bioethanol production.

Finally, the physicochemical properties of the distilled ethanol confirmed the effectiveness of downstream processing. The density (0.812 g/cm^3) and flash point (14°C) are close to those of commercial ethanol fuels, indicating successful enrichment through distillation. However, slight deviations from pure ethanol values suggest the presence of residual water, which is expected in single-stage distillation systems. This highlights the importance of integrating efficient purification techniques, such as fractional distillation or dehydration, to achieve fuel-grade ethanol. In general, this study demonstrates that the integration of fungal delignification, optimized fermentation conditions, and MIL-100(Fe)-based immobilized yeast can produce bioethanol from lignocellulosic biomass with competitive performance. Although the ethanol yield remains moderate, the system offers significant advantages in terms of sustainability, reusability, and process integration, providing a promising platform for further development and scale-up.

Future work should focus on improving ethanol yield through process optimization, such as enhancing enzymatic hydrolysis efficiency, reducing the formation of inhibitory compounds, and optimizing nutrient supplementation during fermentation. In addition, alternative process configurations beyond SHF are strongly recommended, particularly simultaneous saccharification and fermentation (SSF) or simultaneous saccharification and co-fermentation (SSCF), which can improve overall efficiency by reducing product inhibition and enabling better integration of enzymatic hydrolysis and fermentation steps. These approaches have been widely reported to yield higher ethanol concentrations compared to SHF systems. Furthermore, the application of advanced separation techniques, including multi-stage

distillation or dehydration processes, is recommended to obtain higher-purity ethanol. Further studies on the long-term performance of immobilized yeast and the structural integrity of the MIL-100(Fe) matrix are required to enable industrial application.

5. Conclusions

This study demonstrates the effective use of *C. caperata* for laccase production to facilitate delignification of Taberau (*Phragmites australis*) biomass, enhancing its cellulose accessibility for enzymatic hydrolysis and subsequent bioethanol production. The fungal pre-treatment reduced lignin content significantly, which in turn improved sugar release during hydrolysis. Furthermore, yeast cells immobilized on MIL-100(Fe) exhibited enhanced ethanol production compared to free yeast cells, with optimal yields achieved under specific conditions of yeast dosage and fermentation time. The immobilized yeast system retained structural integrity and effectively consumed sugars, demonstrating its potential for sustainable bioethanol production. However, ethanol yield decreased over successive reuse cycles, indicating the necessity for further optimization. The combined use of fungal pre-treatment and immobilized yeast fermentation offers a viable approach to improve lignocellulosic biomass conversion into biofuels for both eco-friendly and industrial applications.

Declarations

Acknowledgements

The authors would like to express their sincere appreciation to colleagues and collaborators for their valuable support and contributions throughout this study.

Funding

This research was financially supported by the Ministry of Research, Technology, and Higher Education, Indonesia under Grant No. 1000/UN24.13/AL.O4/2024.

Author Contributions

TAA was responsible for the methodology, investigation, formal analysis, data curation, and drafting the original manuscript. **YY** and **YA** contributed to the investigation, methodology, formal analysis, and data curation. **WJ**, **LT**, and **EJK** involved to the formal analysis, data curation, and preparing visualizations. **RA** provided to the conceptualization, methodology, validation, supervision, and project administration, as well as contributed to the manuscript review and editing. All authors have read and approved the final manuscript.

Data availability

All data are included in the manuscript, and additional data can be available upon request.

Declarations of Conflic of interest

The authors declare that there is no conflict of interest regarding the publication of this manuscript. All authors have contributed significantly to the research and preparation of the manuscript, and no competing financial, professional, or personal interests could have influenced the work or its interpretation.

References

1. Hasan, M. H., Mahlia, T. M. I., & Nur, H. (2012). A review on energy scenario and sustainable energy in Indonesia. *Renewable and Sustainable Energy Reviews*, *16*(4), 2316–2328. https://doi.org/10.1016/j.rser.2011.12.007
2. United Nations Department of Economic and Social Affairs, P. D. (2022). W. P. P. 2022: S. of R., Raimi, D., Zhu, Y., Newell, R. G., Prest, B. C., & Bergman, A. (2022). *Global Energy Outlook 2023: Sowing the Seeds of an Energy Transition*. *United Nation*. Retrieved from http://dx.doi.org/10.17605/OSF.IO/W3B4Z%0Awww.un.org/development/ desa/pd/.
3. Holtom, B. (2004). Fossil fuels, alternative energy and economic growth. *Journal of Nursing Administration*, *34*(5), 216–227.
4. Abas, N., Kalair, A., & Khan, N. (2015). Review of fossil fuels and future energy technologies. *Futures*, *69*, 31–49. https://doi.org/10.1016/j.futures.2015.03.003
5. Wang, J., & Azam, W. (2024). Natural resource scarcity, fossil fuel energy consumption, and total greenhouse gas emissions in top emitting countries. *Geoscience Frontiers*, *15*(2), 2024. https://doi.org/10.1016/j.gsf.2023.101757
6. Merritt, H., & Barragán-Ocaña, A. (2023). The impact of market factors on the development of eco-friendly energy technologies: the case of bioethanol. *Clean Technologies and Environmental Policy*, *25*(2), 313–321. https://doi.org/10.1007/s10098-021-02225-6
7. Ripple, W. J., Wolf, C., Gregg, J. W., Rockström, J., Mann, M. E., Oreskes, N., … Crowther, T. W. (2024). The 2024 state of the climate report : Perilous times, 1–13.
8. Rajak, R. C., & Banerjee, R. (2018). An eco-friendly process integration for second generation bioethanol production from laccase delignified Kans grass. *Energy Conversion and Management*, *157*, 364–371. https://doi.org/10.1016/j.enconman.2017.11.060
9. Lamichhane, G., Acharya, A., Poudel, D. K., Aryal, B., Gyawali, N., Niraula, P., … Parajuli, N. (2021). Recent advances in bioethanol production from Lignocellulosic biomass. *International Journal of Green Energy*, *18*(7), 731–744. https://doi.org/10.1080/15435075.2021.1880910
10. Kordala, N., Walter, M., Brzozowski, B., & Lewandowska, M. (2024). 2G-biofuel ethanol: an overview of crucial operations, advances and limitations. *Biomass Conversion and Biorefinery*, *14*(3), 2983–3006. https://doi.org/10.1007/s13399-022-02861-y
11. Limayem, A., & Ricke, S. C. (2012). Lignocellulosic biomass for bioethanol production: Current perspectives, potential issues and future prospects. *Progress in Energy and Combustion Science*,

38(4), 449–467. https://doi.org/10.1016/j.pecs.2012.03.002

12. Das, N., Jena, P. K., Padhi, D., Kumar Mohanty, M., & Sahoo, G. (2023). A comprehensive review of characterization, pretreatment and its applications on different lignocellulosic biomass for bioethanol production. *Biomass Conversion and Biorefinery*, *13*(2), 1503–1527. https://doi.org/10.1007/s13399-021-01294-3
13. Persson, T., Garcia, A. G. Y., Paz, J. O., Fraisse, C. W., & Hoogenboom, G. (2010). Reduction in greenhouse gas emissions due to the use of bio-ethanol from wheat grain and straw produced in the south-eastern USA. *Journal of Agricultural Science*, *148*(5), 511–527. https://doi.org/10.1017/S0021859610000316
14. Abdul Kareem Joyia, M., Ahmad, M., Chen, Y. F., Mustaqeem, M., Ali, A., Abbas, A., & Ashraf Gondal, M. (2024). Trends and advances in sustainable bioethanol production technologies from first to fourth generation: A critical review. *Energy Conversion and Management*, *321*, 2024. https://doi.org/10.1016/j.enconman.2024.119037
15. Cavalaglio, G., Gelosia, M., Ingles, D., Pompili, E., D'Antonio, S., & Cotana, F. (2016). Response surface methodology for the optimization of cellulosic ethanol production from Phragmites australis through pre-saccharification and simultaneous saccharification and fermentation. *Industrial Crops and Products*, *83*, 431–437. https://doi.org/10.1016/j.indcrop.2015.12.089
16. Cotana, F., Cavalaglio, G., Pisello, A. L., Gelosia, M., Ingles, D., & Pompili, E. (2015). Sustainable ethanol production from common reed (Phragmites australis) through simultaneuos saccharification and fermentation. *Sustainability (Switzerland)*, *7*(9), 12149–12163. https://doi.org/10.3390/su70912149
17. Tozluoglu, A. (2018). Bioethanol production from common reed (Phragmites australis): Enzymatic hydrolysis and fermentation. *Romanian Biotechnological Letters*, *23*(2), 13473–13478.
18. Köbbing, J. F., Thevs, N., & Zerbe, S. (2013). The utilisation of reed (Phragmites australis): a review. *Mires and Peat*, *13*, 1–14.
19. Sathitsuksanoh, N., Zhu, Z., Templeton, N., Rollin, J. A., Harvey, S. P., & Zhang, Y. H. P. (2009). Saccharification of a potential bioenergy crop, phragmites australis (Common Reed), by lignocellulose fractionation followed by enzymatic hydrolysis at decreased cellulase loadings. *Industrial and Engineering Chemistry Research*, *48*(13), 6441–6447. https://doi.org/10.1021/ie900291s
20. Gao, K., Boiano, S., Marzocchella, A., & Rehmann, L. (2014). Cellulosic butanol production from alkali-pretreated switchgrass (Panicum virgatum) and phragmites (Phragmites australis). *Bioresource Technology*, *174*, 176–181. https://doi.org/10.1016/j.biortech.2014.09.152
21. Elhaak, Mohsen, Hamada, & El-Gebaly. (2015). Biofuel Production From Phragmites Australis (Cav .) and Typha Domingensis (Pers.) Plants of Burullus Lake. *J. Exp. Biol. (Bot.)*, *11*(2), 237–243. Retrieved from http://my.ejmanger.com/ejeb/
22. Suryadi, H., Judono, J. J., Putri, M. R., Eclessia, A. D., Ulhaq, J. M., Agustina, D. N., & Sumiati, T. (2022). Biodelignification of lignocellulose using ligninolytic enzymes from white-rot fungi. *Heliyon*,

8(2), e08865. https://doi.org/10.1016/j.heliyon.2022.e08865

23. Isikhuemhen, O. S., Mikiashvili, N. A., Senwo, Z. N., & Ohimain, E. I. (2014). Biodegradation and Sugar Release from Canola Plant Biomass by Selected White Rot Fungi. *Advances in Biological Chemistry*, *04*(06), 395–406. https://doi.org/10.4236/abc.2014.46045
24. De La Torre, M., Martín-Sampedro, R., Fillat, Ú., Eugenio, M. E., Blánquez, A., Hernández, M., … Ibarra, D. (2017). Comparison of the efficiency of bacterial and fungal laccases in delignification and detoxification of steam-pretreated lignocellulosic biomass for bioethanol production. *Journal of Industrial Microbiology and Biotechnology*, *44*(11), 1561–1573. https://doi.org/10.1007/s10295-017-1977-1
25. Plácido, J., & Capareda, S. (2015). Ligninolytic enzymes: A biotechnological alternative for bioethanol production. *Bioresources and Bioprocessing*, *2*(1). https://doi.org/10.1186/s40643-015-0049-5
26. Loi, M., Glazunova, O., Fedorova, T., Logrieco, A. F., & Mulè, G. (2021). Fungal laccases: The forefront of enzymes for sustainability. *Journal of Fungi*, *7*(12), 1–25. https://doi.org/10.3390/jof7121048
27. Roth, S., & Spiess, A. C. (2015). Laccases for biorefinery applications: a critical review on challenges and perspectives. *Bioprocess and Biosystems Engineering*, *38*(12), 2285–2313. https://doi.org/10.1007/s00449-015-1475-7
28. Liong, Y. Y., Halis, R., Lai, O. M., & Mohamed, R. (2012). Conversion of lignocellulosic biomass from grass to bioethanol using materials pretreated with alkali and the white rot fungus, Phanerochaete chrysosporium. *BioResources*, *7*(4), 5500–5513. https://doi.org/10.15376/biores.7.4.5500-5513
29. López-Abelairas, M., Álvarez Pallín, M., Salvachúa, D., Lú-Chau, T., Martínez, M. J., & Lema, J. M. (2013). Optimisation of the biological pretreatment of wheat straw with white-rot fungi for ethanol production. *Bioprocess and Biosystems Engineering*, *36*(9), 1251–1260. https://doi.org/10.1007/s00449-012-0869-z
30. Castoldi, R., Bracht, A., de Morais, G. R., Baesso, M. L., Correa, R. C. G., Peralta, R. A., … Peralta, R. M. (2014). Biological pretreatment of Eucalyptus grandis sawdust with white-rot fungi: Study of degradation patterns and saccharification kinetics. *Chemical Engineering Journal*, *258*, 240–246. https://doi.org/10.1016/j.cej.2014.07.090
31. Ding, C., Wang, X., & Li, M. (2019). Evaluation of six white-rot fungal pretreatments on corn stover for the production of cellulolytic and ligninolytic enzymes, reducing sugars, and ethanol. *Applied Microbiology and Biotechnology*, *103*(14), 5641–5652. https://doi.org/10.1007/s00253-019-09884-y
32. Agnestisia, R., Panjaitan, D., Erdene-ochir, T., & Nion, Y. A. (2024). Decolorization of Rhodamine B by the white rot fungus Coriolopsis caperata isolated from Central Kalimantan Forest. *BIO Web of Conferences*, *134*, 06011.
33. Agnestisia, R., Karelius, K., Oksal, E., & Nion, Y. A. (2025). Decolorization of textile dyes with crude ligninolytic enzymes from Coriolopsis caperata. *Jurnal Bioteknologi dan Biosains Indonesia*, *12*(1), 104–118.

34. Kallel, F., Neifar, M., Kacem, I., & Ellouz Chaabouni, S. (2024). Optimization of enzymatic hydrolysis and fermentation of bleached garlic straw for bioethanol production. *Journal of Material Cycles and Waste Management*, *26*(5), 2880–2895. https://doi.org/10.1007/s10163-024-02016-3
35. Averheim, A., Stagge, S., Jönsson, L. J., Larsson, S. H., & Thyrel, M. (2024). Separate hydrolysis and fermentation of softwood bark pretreated with 2-naphthol by steam explosion. *Biotechnology for Biofuels and Bioproducts*, *17*(1), 1–10. https://doi.org/10.1186/s13068-024-02552-y
36. Drissen, R. E. T., Maas, R. H. W., Tramper, J., & Beeftink, H. H. (2009). Modelling ethanol production from cellulose: Separate hydrolysis and fermentation versus simultaneous saccharification and fermentation. *Biocatalysis and Biotransformation*, *27*(1), 27–35. https://doi.org/10.1080/10242420802564358
37. Bhadana, B., & Chauhan, M. (2016). Bioethanol Production Using Saccharomyces cerevisiae with Different Perspectives: Substrates, Growth Variables, Inhibitor Reduction and Immobilization. *Fermentation Technology*, *5*(2), 2–5. https://doi.org/10.4172/2167-7972.1000131
38. Kumoro, A. C., Damayanti, A., Bahlawan, Z. A. S., Melina, M., & Puspawati, H. (2021). Bioethanol production from oil palm empty fruit bunches using saccharomyces cerevisiae immobilized on sodium alginate beads. *Periodica Polytechnica Chemical Engineering*, *65*(4), 493–504. https://doi.org/10.3311/PPch.16775
39. Mariam, I., Manzoor, K., Ali, S., & Ikram-Ul-Haq. (2009). Enhanced production of ethanol from free and immobilized Saccharomyces cerevisiae under stationary culture. *Pakistan Journal of Botany*, *41*(2), 821–833.
40. Md Zain, M., Kofli, N. T., & Yahya, A. S. R. S. (2011). Bioethanol Production by Calcium Alginate-Immobilised St1 Yeast System: Effects of Size of Beads, Ratio and Concentration. *IIUM Engineering Journal*, *12*(4), 11–19. https://doi.org/10.31436/iiumej.v12i4.159
41. Gökgöz, M., & Yiğitoğlu, M. (2011). Immobilization of Saccharomyces cerevisiae on to modified carboxymethylcellulose for production of ethanol. *Bioprocess and Biosystems Engineering*, *34*(7), 849–857. https://doi.org/10.1007/s00449-011-0535-x
42. Liang, K., Richardson, J. J., Doonan, C. J., Mulet, X., Ju, Y., Cui, J., … Falcaro, P. (2017). An Enzyme-Coated Metal–Organic Framework Shell for Synthetically Adaptive Cell Survival. *Angewandte Chemie - International Edition*, *56*(29), 8510–8515. https://doi.org/10.1002/anie.201704120
43. Sun, H., Li, Y., Yu, S., & Liu, J. (2020). Metal-organic frameworks (MOFs) for biopreservation: From biomacromolecules, living organisms to biological devices. *Nano Today*, *35*, 2024. https://doi.org/10.1016/j.nantod.2020.100985
44. Liang, S., Wu, X. L., Xiong, J., Zong, M. H., & Lou, W. Y. (2020). Metal-organic frameworks as novel matrices for efficient enzyme immobilization: An update review. *Coordination Chemistry Reviews*, *406*, 213149. https://doi.org/10.1016/j.ccr.2019.213149
45. Hu, J., Yuan, X., Wang, C., Shao, X., Yang, B., Abdul Razzaq, A., … Peng, Y. (2020). Self-Phosphorization of MOF-Armored Microbes for Advanced Energy Storage. *Small*, *16*(24), 1–9. https://doi.org/10.1002/smll.202000755

46. Zhong, G., Liu, D., & Zhang, J. (2018). Applications of Porous Metal-Organic Framework MIL-100(M) (M = Cr, Fe, Sc, Al, V). *Crystal Growth and Design*, *18*(12), 7730–7744. https://doi.org/10.1021/acs.cgd.8b01353
47. Zhang, F., Shi, J., Jin, Y., Fu, Y., Zhong, Y., & Zhu, W. (2015). Facile synthesis of MIL-100(Fe) under HF-free conditions and its application in the acetalization of aldehydes with diols. *Chemical Engineering Journal*, *259*, 183–190. https://doi.org/10.1016/j.cej.2014.07.119
48. Leonowicz, A., & Gzrywnowicz, K. (1981). Quantitative estimation of laccase forms in some white-rot fungi using syringaldazine as a substrate. *Enzyme and Microbial Technology*, *3*, 55–58.
49. Ghose, T. K. (1987). Measurement of cellulase activities, *59*(2), 257–268. https://doi.org/doi:10.1351/pac198759020257
50. Sivakumar, R., Rajendran, R., Balakumar, C., Tamilvendan, M., & R. Sivakumar, R. Rajendran, C. Balakumar, M. T. (2010). Isolation , Screening and Optimization of Production Medium for Thermostable Laccase Production from Ganoderma sp. *International Journal of Engineering Science*, *2*(12), 7133–7141. Retrieved from http://www.ijest.info/docs/IJEST10-02-12-241.pdf
51. Couto, S. R., Gundín, M., Lorenzo, M., & Sanromán, M. Á. (2002). Screening of supports and inducers for laccase production by Trametes versicolor in semi-solid-state conditions. *Process Biochemistry*, *38*(2), 249–255. https://doi.org/10.1016/S0032-9592(02)00087-0
52. Patrick, F., Mtui, G., Mshandete, A., & Kivaisi, A. (2010). Tanzania Journal of Science Peroxidase and Laccase in Submerged Cultures of, *36*.
53. Hadibarata, T., & Yuniarto, A. (2020). Biodegradation of polycyclic aromatic hydrocarbons by high-laccase basidiomycetes fungi isolated from tropical forest of Borneo. *Biocatalysis and Agricultural Biotechnology*, *28*(July), 101717. https://doi.org/10.1016/j.bcab.2020.101717
54. Wan, C., & Li, Y. (2011). Effectiveness of microbial pretreatment by Ceriporiopsis subvermispora on different biomass feedstocks. *Bioresource Technology*, *102*(16), 7507–7512. https://doi.org/10.1016/j.biortech.2011.05.026
55. Bagewadi, Z. K., Mulla, S. I., & Ninnekar, H. Z. (2017). Optimization of laccase production and its application in delignification of biomass. *International Journal of Recycling of Organic Waste in Agriculture*, *6*(4), 351–365. https://doi.org/10.1007/s40093-017-0184-4
56. Gupta, R., Mehta, G., Khasa, Y. P., & Kuhad, R. C. (2011). Fungal delignification of lignocellulosic biomass improves the saccharification of cellulosics. *Biodegradation*, *22*(4), 797–804. https://doi.org/10.1007/s10532-010-9404-6
57. Pasaribu, M. H., Karelius, K., Ramdhani, E. P., Agnestisia, R., Pereiz, Z., & Toepak, E. P. (2023). Synthesis of Mil-100(Fe)@Fe3O4 Composite using Zircon Mining Magnetic Waste as an Adsorbent for Methylene Blue Dye. *BIO Web of Conferences*, *70*. https://doi.org/10.1051/bioconf/20237002010
58. Permyakova, A., Kakar, A., Bachir, J., Gkaniatsou, E., Haye, B., Menguy, N., … Sicard, C. (2022). In Situ Synthesis of a Mesoporous MIL-100 (Fe) Bacteria Exoskeleton. *ACS Materials Letters*, *5*(1), 79–84.
59. Chávez, A. M., Rey, A., López, J., Álvarez, P. M., & Beltrán, F. J. (2021). Critical aspects of the stability and catalytic activity of MIL-100(Fe) in different advanced oxidation processes. *Separation and*

Purification Technology, *255*(June 2020), 117660. https://doi.org/10.1016/j.seppur.2020.117660

60. Han, L., Qi, H., Zhang, D., Ye, G., Zhou, W., Hou, C., … Sun, Y. (2017). A facile and green synthesis of MIL-100(Fe) with high-yield and its catalytic performance. *New Journal of Chemistry*, *41*(22), 13504–13509. https://doi.org/10.1039/c7nj02975f
61. Zhang, X., Zhang, X., He, W., Sun, C., Ma, J., Yuan, J., & Du, X. (2013). High-performance mesoporous LiFePO4 from Baker's yeast. *Colloids and Surfaces B: Biointerfaces*, *103*(October 2012), 114–120. https://doi.org/10.1016/j.colsurfb.2012.10.002
62. Lyu, F., Zhang, Y., Zare, R. N., Ge, J., & Liu, Z. (2014). One-pot synthesis of protein-embedded metal-organic frameworks with enhanced biological activities. *Nano Letters*, *14*(10), 5761–5765. https://doi.org/10.1021/nl5026419
63. Yang, W., Liang, W., O'Dell, L. A., Toop, H. D., Maddigan, N., Zhang, X., … Huang, J. (2021). Insights into the Interaction between Immobilized Biocatalysts and Metal-Organic Frameworks: A Case Study of PCN-333. *JACS Au*, *1*(12), 2172–2181. https://doi.org/10.1021/jacsau.1c00226
64. Mulko, L., Rivarola, C. R., Barbero, C. A., & Acevedo, D. F. (2016). Bioethanol production by reusable Saccharomyces cerevisiae immobilized in a macroporous monolithic hydrogel matrices. *Journal of Biotechnology*, *233*, 56–65. https://doi.org/10.1016/j.jbiotec.2016.07.004
65. Zabed, H., Sahu, J. N., Suely, A., Boyce, A. N., & Faruq, G. (2017). Bioethanol production from renewable sources: Current perspectives and technological progress. *Renewable and Sustainable Energy Reviews*, *71*, 475–501. https://doi.org/10.1016/j.rser.2016.12.076
66. Kourkoutas, Y., Bekatorou, A., Banat, I. M., Marchant, R., & Koutinas, A. A. (2004). Immobilization technologies and support materials suitable in alcohol beverages production: A review. *Food Microbiology*, *21*(4), 377–397. https://doi.org/10.1016/j.fm.2003.10.005
67. Shen, H. Y., Moonjai, N., Verstrepen, K. J., & Delvaux, F. R. (2003). Impact of attachment immobilization on yeast physiology and fermentation performance. *Journal of the American Society of Brewing Chemists*, *61*(2), 79–87. https://doi.org/10.1094/asbcj-61-0079
68. Bai, F. W., Anderson, W. A., & Moo-Young, M. (2008). Ethanol fermentation technologies from sugar and starch feedstocks. *Biotechnology Advances*, *26*(1), 89–105. https://doi.org/10.1016/j.biotechadv.2007.09.002
69. Onaifo, J. O., Ikhuoria, E. U., Omorogbe, S. O., Agbonlahor, O. G., & Ifijen, I. H. (2016). Coconut Pit an Alternative Source of Producing Renewable Material (Bioethanol). *Journal of Applied Chemical Science International*, *6*(2), 80–84.
70. Jönsson, L. J., & Martín, C. (2016). Pretreatment of lignocellulose: Formation of inhibitory by-products and strategies for minimizing their effects. *Bioresource Technology*, *199*, 103–112. https://doi.org/10.1016/j.biortech.2015.10.009
71. Jin, X., Song, J., & Liu, G. Q. (2020). Bioethanol production from rice straw through an enzymatic route mediated by enzymes developed in-house from Aspergillus fumigatus. *Energy*, *190*(xxxx), 116395. https://doi.org/10.1016/j.energy.2019.116395

72. Shen, F., Kumar, L., Hu, J., & Saddler, J. N. (2011). Evaluation of hemicellulose removal by xylanase and delignification on SHF and SSF for bioethanol production with steam-pretreated substrates. *Bioresource Technology*, *102*(19), 8945–8951. https://doi.org/10.1016/j.biortech.2011.07.028
73. Pooja, N. S., Sajeev, M. S., Jeeva, M. L., & Padmaja, G. (2018). Bioethanol production from microwave-assisted acid or alkali-pretreated agricultural residues of cassava using separate hydrolysis and fermentation (SHF). *3 Biotech*, *8*(1), 1–12. https://doi.org/10.1007/s13205-018-1095-4
74. Singh, A., Sharma, P., Saran, A. K., Singh, N., & Bishnoi, N. R. (2013). Comparative study on ethanol production from pretreated sugarcane bagasse using immobilized Saccharomyces cerevisiae on various matrices. *Renewable Energy*, *50*, 488–493. https://doi.org/10.1016/j.renene.2012.07.003

Figures

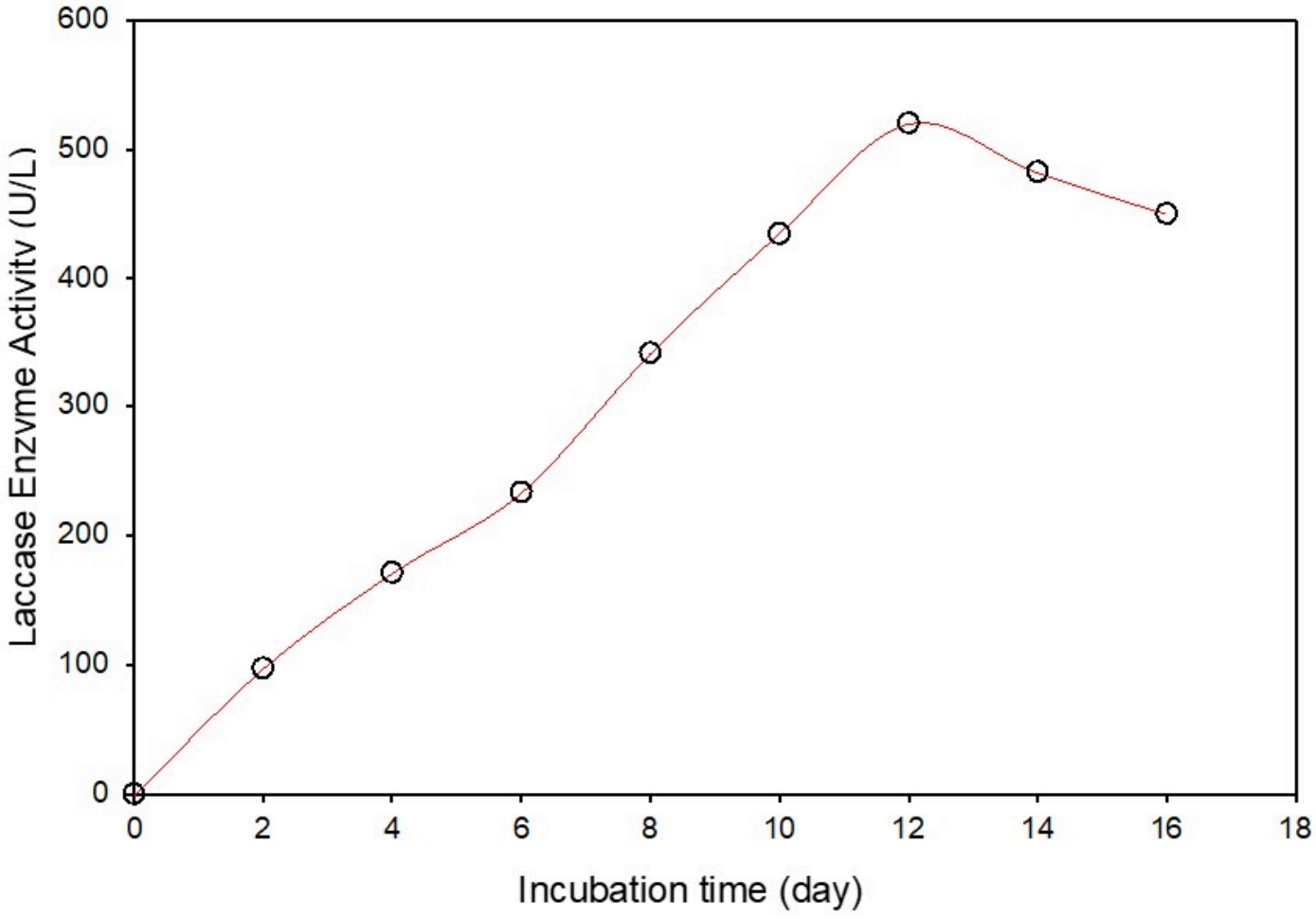


Figure 1

Effect of incubation time on laccase production

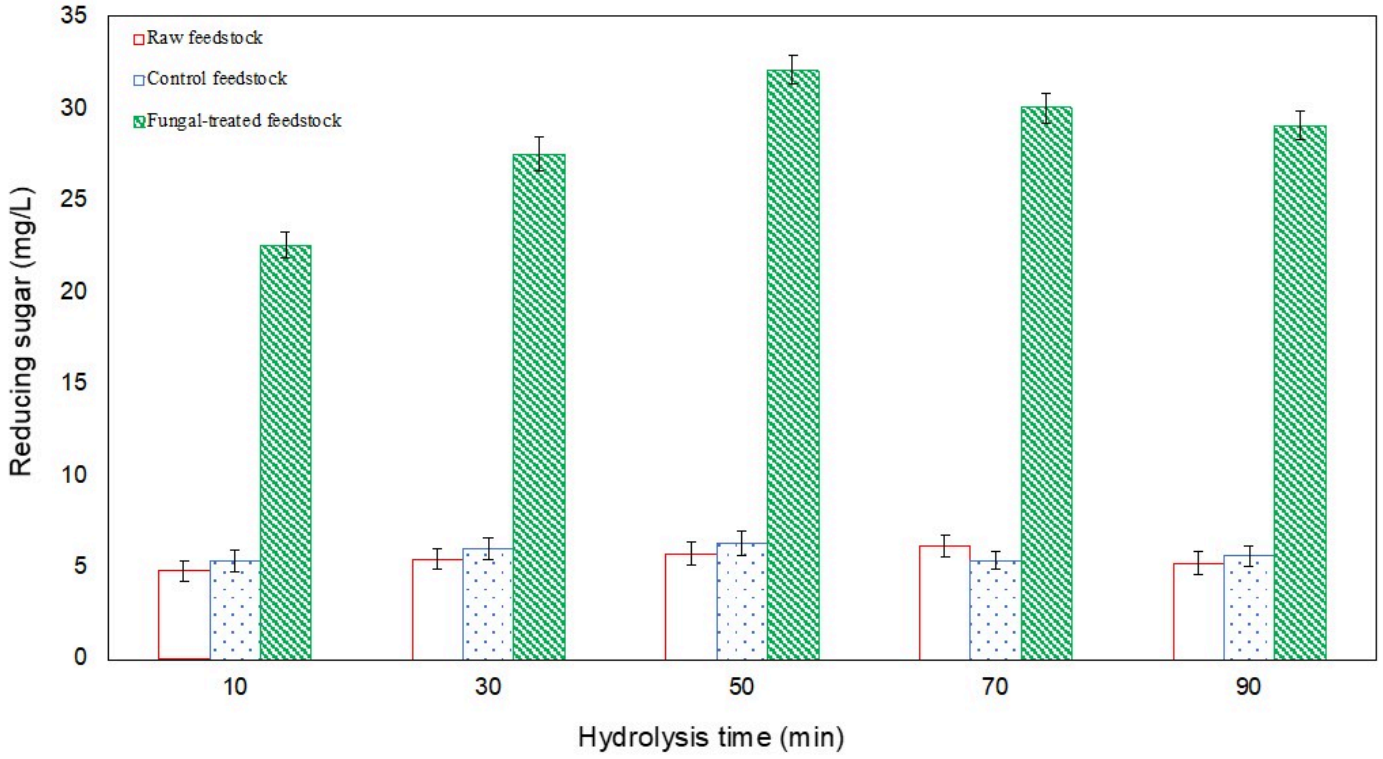


Figure 2

Effect of hydrolysis time on reducing sugar concentration

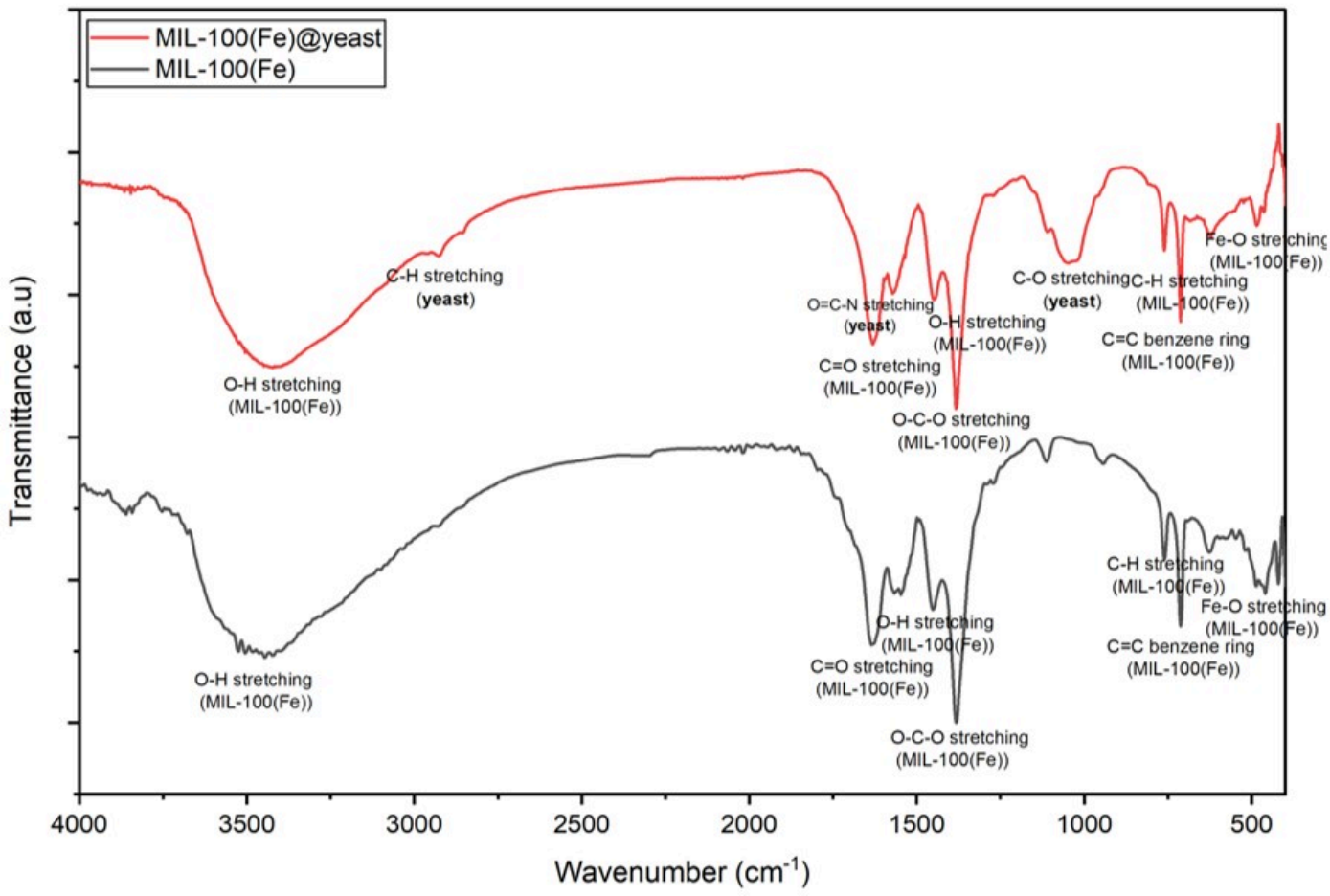


Figure 3

FTIR spectra of MIL-100(Fe) and MIL-100(Fe)@yeast

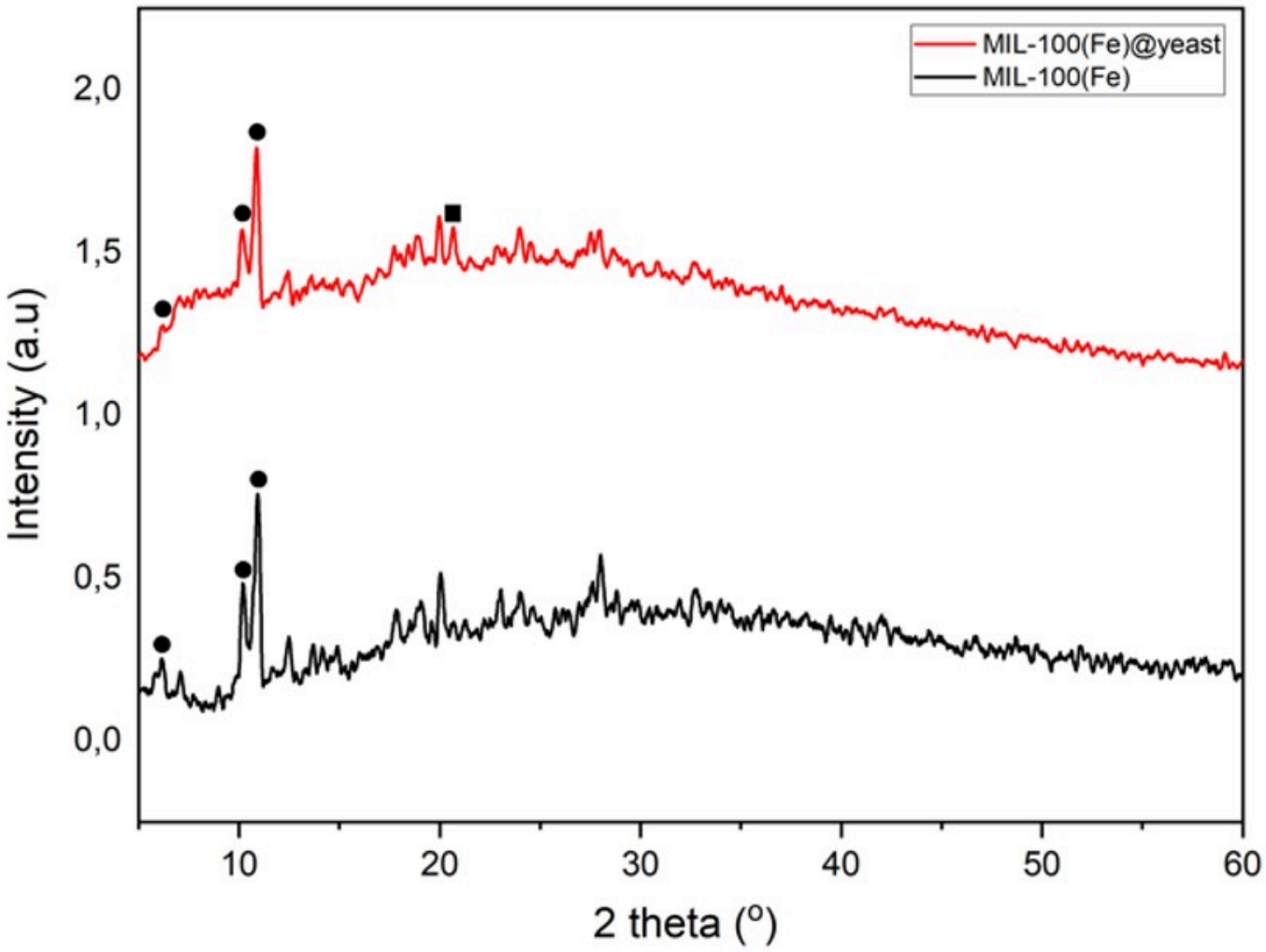


Figure 4

FTIR Diffractogram of MIL-100(Fe) and MIL-100(Fe)@yeast.

Note: ●, MIL-100(Fe) and ■, yeast

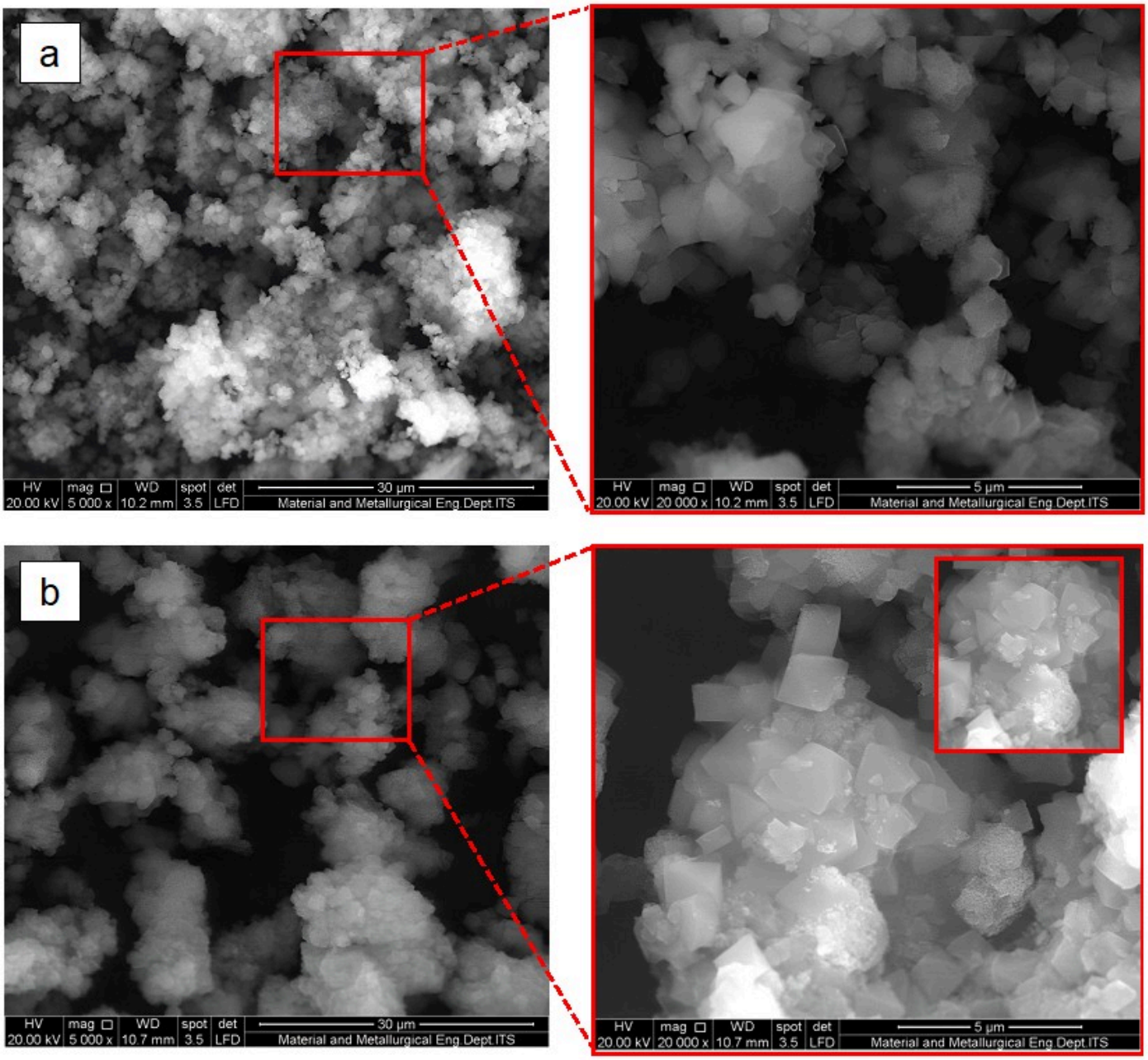


Figure 5

SEM images of (a) MIL-100(Fe) and (b) MIL-100(Fe)@yeast

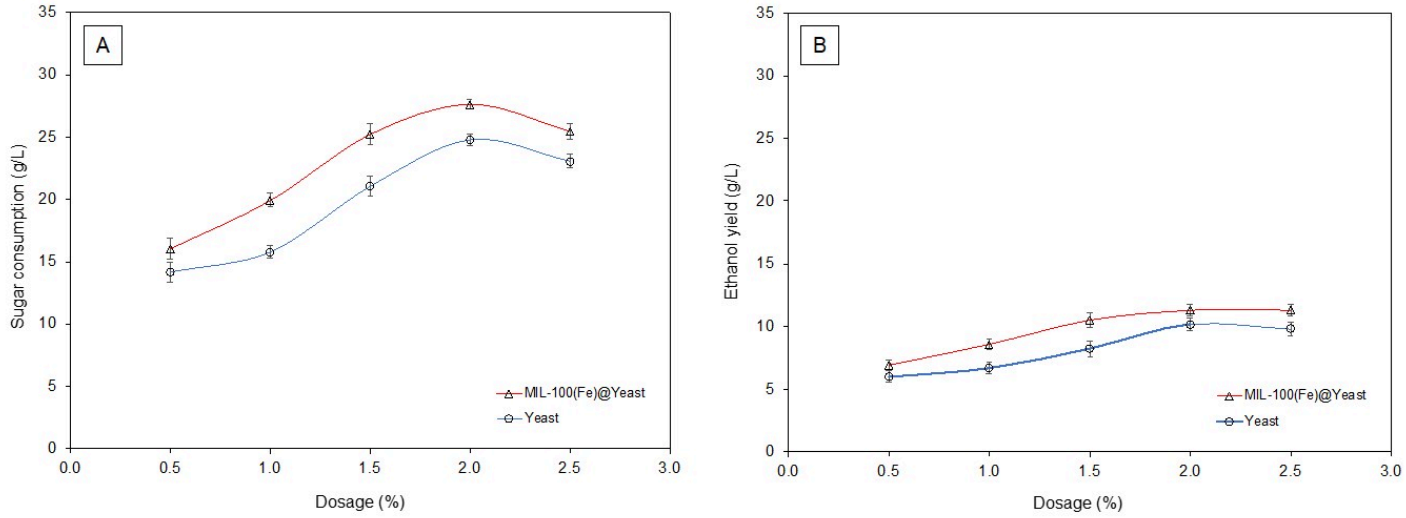


Figure 6

Effect of different free and immobilized yeast dosage on (a) sugar consumption and (b) ethanol production

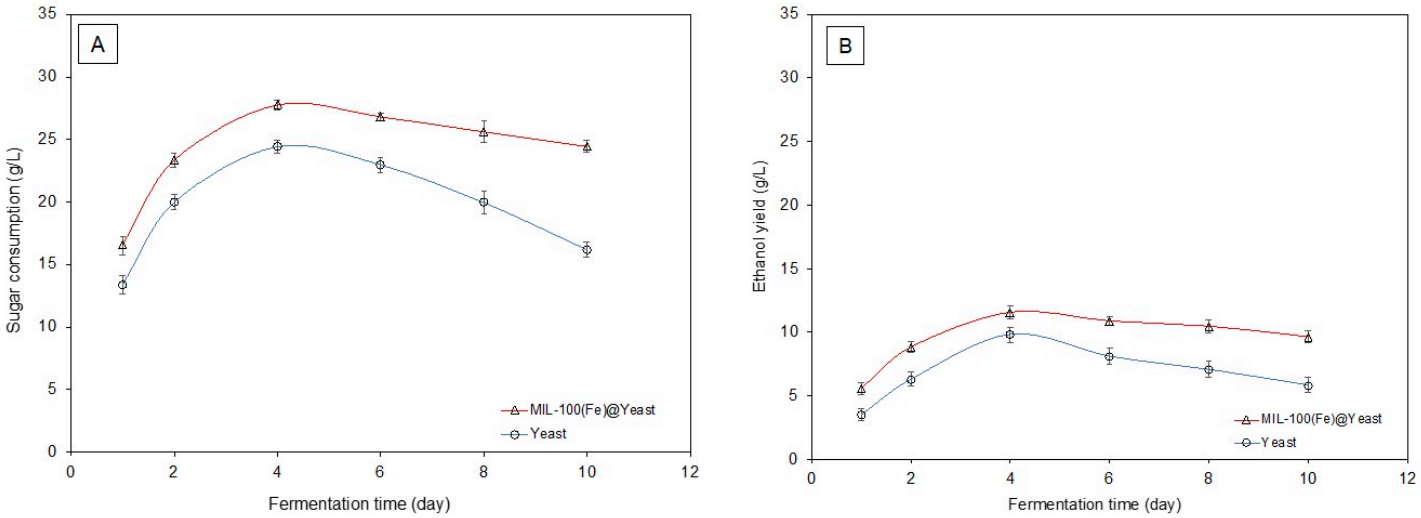


Figure 7

Effect of different fermentation time on (a) sugar consumption and (b) ethanol production

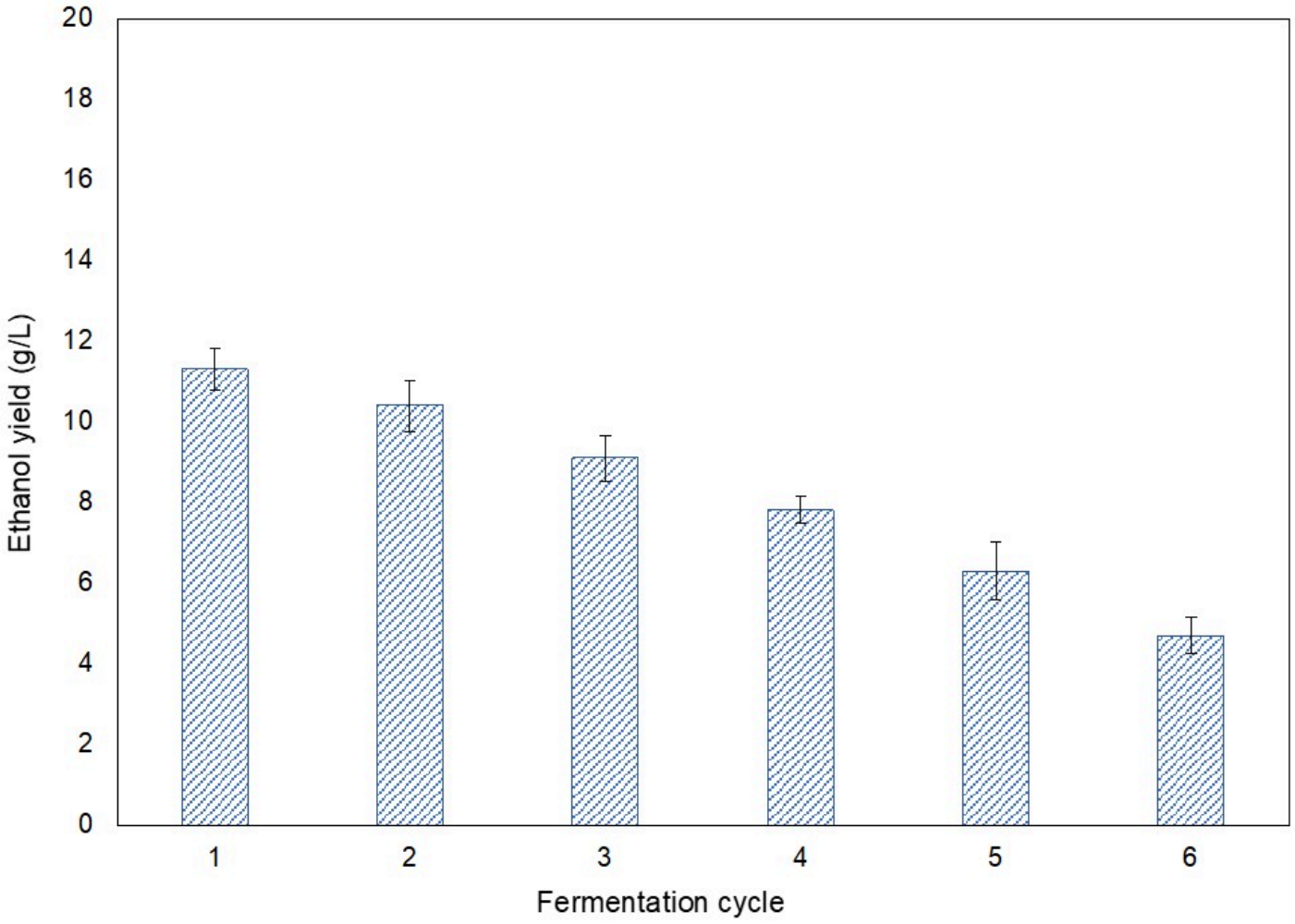


Figure 8

Reusability of MIL-100(Fe)@yeast

Supplementary Files

This is a list of supplementary files associated with this preprint. Click to download.

- Graphicalabstract.jpg